Fluid flow and thermal analysis of Al_2O_3-water nanofluid in multi-microchannel heat sinks

Isabelle Guimarães da Silva[1], João Batista Campos Silva[2], Elaine Maria Cardoso[1,2]

[1]*UNESP - São Paulo State University, Câmpus of São João da Boa Vista, São João da Boa Vista, SP 13876-750, Brazil;*
isabelle.g.silva@unesp.br
[2]*UNESP - São Paulo State University, School of Engineering, Post-Graduation Program in Mechanical Engineering, Av. Brasil, 56, Ilha Solteira, SP 15385-000, Brazil;*
campos.silva@unesp.br, elaine.cardoso@unesp.br

Abstract. This work analyzes different working fluids (DI-water and Al_2O_3-water based nanofluid) flowing in a copper microchannel heat sink consisting of 20 parallel rectangular channels of 29.23 mm in length, 1.2 mm in width, and 1.2 mm in height for each microchannel and investigates their influence on the velocity flow field, pressure drop, and heat transfer. The CFD software ANSYS FLUENT 2020 R2® was applied. In the case of Alumina-water nanofluid with an average nanoparticle size of 10 nm, different volume concentrations were used (0.5% and 1 vol.%). A uniform velocity and temperature (293.15 K) were applied at the inlet of the heat sink. The inlet velocity varied from 3.41 to 8.54 m/s, and the Reynolds number based on the hydraulic diameter and inlet velocity varied from 400 to 1000. A heat flux corresponding to 165 W dissipated power for an Intel® Core™ Serie X processor was applied at the bottom surface of the heat sink. It was possible to obtain different temperature distributions, the pressure drop, and the requested pumping power consumption by modifying the working fluid. Comparisons were performed on how the velocity and temperature fields changed according to boundary conditions. The Alumina-water nanofluid provides a more uniform wall-temperature distribution; the nanofluid with the highest concentration has the highest friction factor and the highest Nusselt number regardless of the Reynolds number. The nanofluid thermal behavior with the volumetric concentration increasing is probably due to the fluid thermal conductivity increasing. Even the higher pressure drop observed for the Al_2O_3-water nanofluid, its effect on the pumping power consumption is acceptable (for the highest nanofluid concentration and Reynolds number, the pressure drop is 93.40 kPa corresponding to a pumping power of 3 W). Therefore, the microchannel heat sink and nanofluids seem a plausible solution for the cooling challenge in microscale electronics due to the higher cooling performance.

Keywords: CFD, Fluid flow, Heat Transfer, Nanofluid, Microchannel heat sink.

1 Introduction

Heat sinks are applied in industries aiming to optimize engineering projects in mechanics, aerospace, electronics, and other areas. In order to avoid damage from heat sources that could compromise data and consequently the investments made, heat sink devices are needed for regulating the temperature, occupying minimal space and enabling the components to operate at their maximum efficiency.

Microscale refrigeration systems can cool high-generation electronic devices and appliances since the heat transfer performance of a microchannel-based heat sink is superior to any traditional heat exchanger, according to Murshed and Castro [1]. Considering that the space required for the cooling device of a particular system has great importance, the model to be developed in this work provides wide industrial application.

According to Qu and Mudawar [2], as the diameter of the channel through which the working fluid flows decreases, the surface area-to-volume ratio increases, reducing the overall system size and fluid inventory;

besides, compact heat exchangers can also be manufactured on the scale of compact electronic device processors (e.g., Intel® Core™ processors). Thereby, the association of microchannels and modern refrigerants shows potential for replacing conventional heat sinks in modern high-efficiency electronic devices [3].

The use of microchannel heat sinks is highly applicable with efficient coolants due to its better capacity to efficiently dissipate large quantities of heat generated from electronic devices than conventional heat transfer fluids, such as water or ethylene glycol [4]. The technique that disperses nanoparticles within a conventional coolant (named nanofluids) can enhance the working fluid's effective thermal conductivity, leading to an increase in the heat transfer performance of the cooling system.

The Computational Fluid Dynamics (CFD) methods are robust tools for simulating the fluid flow and thermal behavior, considering that it numerically solves equations regarding fluid flow and heat transfer problems inside a defined geometry. In other words, CFD presents the crucial and fundamental understanding of the parameters such as velocity, pressure and temperature field, providing the most valuable designs and better efficiency of microchannel heat sink devices [5].

The microchannels present a pressure drop (responsible for pump energy consumption used) more significant than the pressure drop in macro channels under the same operating conditions. Qu and Mudawar [6] performed an experimental and numerical study to predict the pressure drop of a heat exchanger based on rectangular microchannels for single-phase flow using water as a refrigerant fluid. The authors observed that the pressure drop decreased with the increased heat flux applied, considering a constant Reynolds number (decrease in water viscosity with increasing temperature). Tan et al. [7] also presented that the design of a multi-microchannel-based heat exchanger should maximize the flow uniformity in the channels improving the thermal and hydrodynamic performance of the heat exchanger.

In this context, the present work aims to numerically study using ANSYS FLUENT 2020 R2® the pressure drop, velocity field and wall temperature of a microchannel heat sink with a single-phase flow of two different coolants (pure water and Al_2O_3-water nanofluid). For the water-based alumina nanofluid, two different concentrations were analyzed (0.5 and 1 vol.%). The motivation lies in applying the developed methods and results to optimize cooling systems applicable to aerospace and electronic fields.

2 Methodology

The methodology consists of defining the input parameters (as the geometry and the heat sink material – copper was applied on all cases); choosing a reference processor for the power supplied to the thermal system; literature information (related to experimental correlations and thermophysical properties of the material and nanofluid); and considerations of the thermal model (including the operation parameters and thermophysical properties).

The Intel® Core™ was chosen as a reference for the processor used in this work. The chosen processor was an Intel® Core™ Serie X processor (with 40 mm^2), with a power supply of 165W (55842 W/m^2) applied at the bottom surface of the proposed heat sink. The manufacturer provides this operational value, and it was based on the TDP (thermal design power), *i.e.,* it represents the amount of heat that needs to be dissipated for the processor to work properly and with better thermal efficiency.

This work is characterized by cooling based on pumping a working fluid through the heat sink geometry, requiring an external pump source. The pumping power is correlated with the system's pressure drop and, in turn, with the flow and working fluid (high flow rates and higher viscosities provide increased pressure drop) and the heat sink's geometry. The analysis comprises one geometry and three cases: Case 1 corresponds to pure water as the working fluid, and the other two cases correspond to Al_2O_3-water based nanofluid (0.5 vol.%, named Case 2 and 1 vol.%, named Case 3).

2.1 Geometric parameters

The same multi-microchannels geometry was used for all three cases (Table 1 and Figure 1 show the heat sink geometry). This geometry was based on Ramos-Alvarado et al. [8]; however, solid domain (copper) and boundary conditions were changed in order to obtain a different and new construction for analysis.

Table 1. Heat sink geometry for all cases analyzed.

Geometric parameters	Cases 1, 2 and 3
Number of channels [-]	20
Number of walls [-]	19
Length of the channels [mm]	29.23
Length of the walls [mm]	29.23
Width of channels [mm]	1.20
Width of the wall [mm]	1.20
Hight of the channels [mm]	1.20
Hight of the inlet/outlet tube [mm]	4.00
Hydraulic diameter [mm]	1.20

Figure 1. Microchannel heat sink geometry in frontal (left) and isometric (right) view.

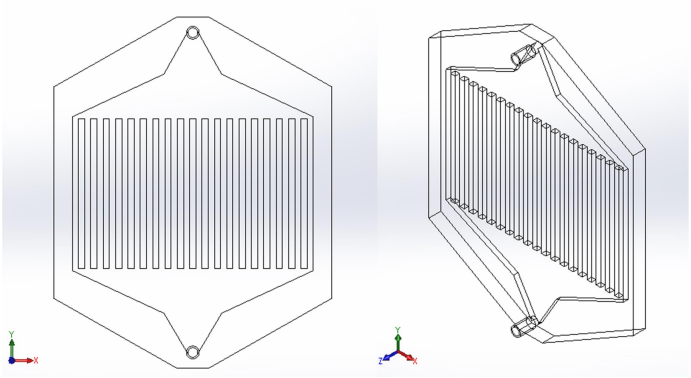

The heat produced by the Intel® Core™ processor will be transferred to the heat sink by conduction and the working fluid by convection. All the other surfaces were considered adiabatic, including the inlet and outlet tube.

2.2 Thermophysical properties

The considerations for developing the thermal model involve steady flow, tridimensional analysis, single-phase and laminar flow, constant thermophysical properties and uniform heat distribution at the bottom of the heat sink. The inlet temperature of the working fluids (water and alumina water-based nanofluid) was considered 293.15K (atmospheric pressure of 98 kPa) and the input power was 165 W.

The properties of the material and both working fluids are presented in Table 2.

Table 2. Thermophysical properties of the working fluids and heat sink material.

Thermophysical properties	Cu	Al_2O_3	DI-water	AL_2O_3-water (0.5 vol.%)	AL_2O_3-water (1 vol.%)
Density [kg/m^3]	8978	3600	998.2	1008.1	1021.1
Specific heat [J/kg K]	381	765	4182	4117.1	4057.7
Thermal conductivity [W/m K]	387.6	36	0.62	0.8926	1.1679
Viscosity [kg/m s]	-	-	0.001003	0.00084047	0.00085112

As the nanofluid thermophysical properties depend on the nanoparticle concentration, the following correlations were used to calculate the density (ρ), dynamic viscosity (μ), and thermal conductivity (k) [4]:

$$\rho_{nf} = \phi\rho_p + (1-\phi)\rho_{bf} \tag{1}$$

$$(\rho \cdot C_p)_{nf} = \phi \cdot (\rho \cdot C_p)_p + (1-\phi) \cdot (\rho \cdot C_p)_{bf} \tag{2}$$

$$\mu_{nf} = \frac{\mu_{bf}}{(1-\phi)^{2.5}} \tag{3}$$

$$\frac{k_{nf}-k_{bf}}{k_{bf}}=\frac{k_p}{k_{bf}}\cdot\left(1+c\frac{u_p\cdot D_p}{\alpha_{bf}}\right)\cdot\frac{D_{bf}}{D_p}\cdot\frac{\phi}{(1-\phi)} \tag{4}$$

where ϕ is the volume concentration; C_p is the specific heat [J/kg K]; *bf* means based-fluid (water); *nf* means nanofluid (alumina water-based); *p* means particle (AL_2O_3); *c* is equal to 25,000, based on [4]; D_p is the particle diameter (in this case, 10 nm); and, D_{bf} is equal to 2.75x10^{-10} m. The u_p parameter corresponds to the Brownian velocity of nanoparticles, and it is given by:

$$u_p=\frac{2\cdot K_b\cdot T}{\pi\cdot\mu_{bf}\cdot D_p^2} \tag{5}$$

where T is the inlet temperature of the nanofluid and K_b is the Boltzmann constant 1.380 x10^{-23} [kg m^2/s^2 K]. The density was kept constant and invariant with the temperature.

2.3 Operation parameters

The following assumptions were made to simplify the problem: steady and laminar flow; no thermo-physical properties variation with temperature; fluid is incompressible; constant solid properties are used, with sidewalls having the adiabatic condition; radiation and viscous dissipation are neglected; and no velocity-slip at the walls. Based on these assumptions, the governing differential equations used to describe the fluid flow and heat transfer in the microchannel are given as:

Conservation of mass (continuity):

$$\nabla.(\rho\boldsymbol{V})=0 \tag{6}$$

Conservation of momentum:

$$\boldsymbol{V}.\nabla(\rho\boldsymbol{V})=-\nabla p+\nabla.(\mu\nabla\boldsymbol{V}) \tag{7}$$

Conservation of energy (Fluid):

$$\boldsymbol{V}.\nabla\left(\rho C_p T_f\right)=\nabla.\left(k_f\nabla T_f\right) \tag{8}$$

The uniform velocity boundary condition was applied at the inlet and a zero static pressure was employed at the outlet. The SIMPLE scheme was used to solve the pressure-velocity coupling. The flow momentum and energy equations are, respectively, solved with a first and second-order upwind scheme. The simulations are performed using a convergence criterion of 10^{-6}.

The hex dominant meshing grid scheme with a free face mesh type combining triangles and quadrilaterals was used to mesh the system, as shown in Figure 2. The mesh was accomplished in the meshing module with minimum mesh orthogonality of 0.329, the maximum aspect ratio of 18.10, and a maximum skewness of 0.67.

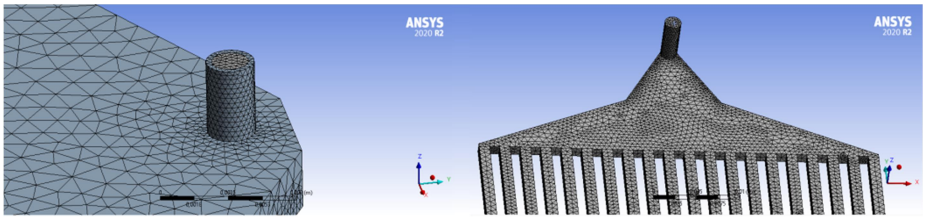

Figure 2. Schematic and computational meshes of the geometrical model.

The average mesh element for the proposed microchannel heat sink was 282,377. The solution achieved convergence after 39 iterations with an average computation time of 10 min.

The Reynolds number is a function of fluid density (ρ); dynamic viscosity (μ); and inlet velocity of the working fluid, and hydraulic diameter (D_h) of the channel:

$$Re=\frac{\rho D_h v_{inlet}}{\mu} \tag{9}$$

The friction factor and pumping power are calculated by Equations (10) and (11):

$$f = \frac{\Delta p_{ch} D_h}{2 L_{ch} \rho v_{inlet}^2} \tag{10}$$

$$P = \Delta p \dot{V} \tag{11}$$

where $\dot{V}$ is the fluid volume flow rate, L_{ch} is the channel length, and Δp is the channel pressure drop.

A grid dependency study was conducted using the wall temperature (in the cross-sectional area of the microchannels) as a criterion to ensure the results are independent of the mesh. Such analysis allows accurate simulation results that do not depend on the quality of the mesh resolution. The procedure is iterative and uses three different meshes (coarse, medium, and fine grid). By the analysis of three different meshes in the present work (with 153,220; 282,377; 455,890 elements), focusing on a heated wall temperature range of a maximum of 2.5 K (less than 10% of the maximum wall temperature, according to Bell Drive [9]), it was noticed that the difference in wall temperature was around 1.2 K between the last two meshes. Hence, a mesh of 282,377 elements was chosen to save computational time.

Validation of Nusselt number and the pressure drop with water and alumina water-based nanofluid is performed by comparing the current results with those obtained by Al-Baghdadi et al. [5]. The modeling results are in good agreement with Al-Baghdadi et al. [5]; for the pressure drop, the mean deviation was 3.4% for water and 7.6% for Al_2O_3-water nanofluid. For the Nusselt number, the mean deviation was 1.3% and 3.1% for water and Al_2O_3-water nanofluid, respectively, indicating the model's reliability used in the current work.

3 Results

Figure 3 shows the wall temperature (corresponding to the temperature of the Intel® processor) for all cases tested as a function of Reynolds number. The heated wall temperature decreases as the Reynolds values increase, as also reported by Mursehd and Castro [1]. This behavior is improved when nanofluids are applied in the cooling system; the higher the nanofluid concentration, the lower the wall temperature [10].

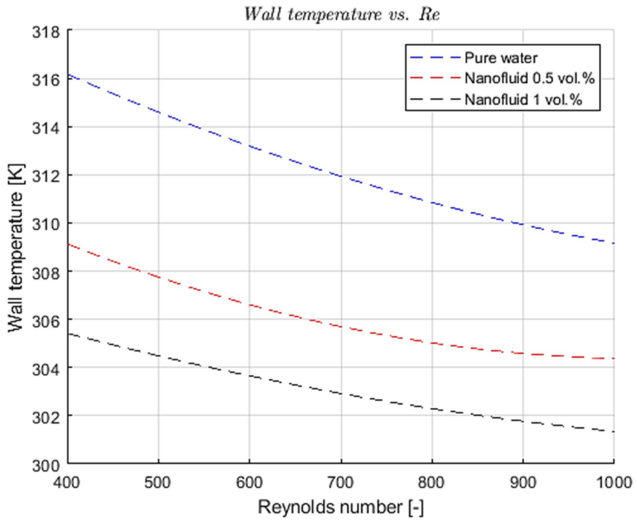

Figure 3. Wall temperature for Cases 1, 2 and 3, respectively.

In order to obtain a clear understanding of the results, Figure 4 presents the wall temperature distribution considering a fixed value of Reynolds number, Re = 800 (corresponding to v_{inlet} of 6.83 m/s), considering three different working fluids: pure water, Al_2O_3-water nanofluid with 0.5 vol.%, Al_2O_3-water nanofluid with 1 vol.%. One may observe that even a smaller concentration of nanoparticles in a base fluid decreases the wall temperature and provides a more uniform wall-temperature distribution, as also reported by Khan et al. [11].

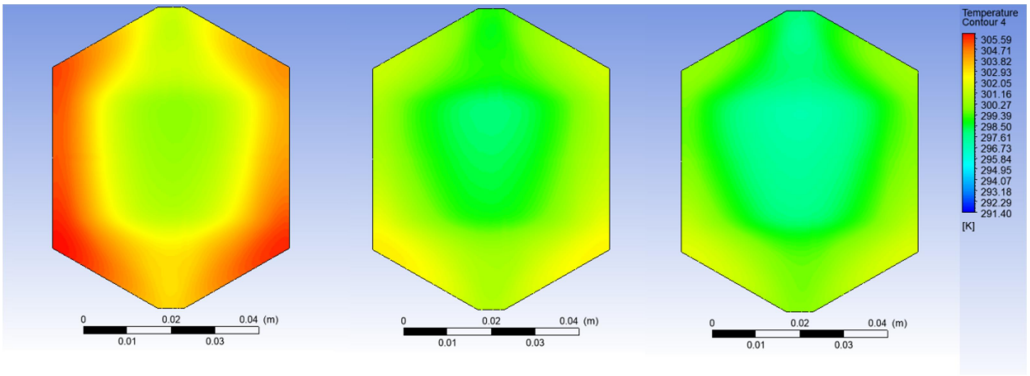

Figure 4. Wall temperature distribution for *Re* = 800 and Cases 1, 2 and 3, respectively.

The nanofluid viscosity depends on the volumetric concentration of nanoparticles [11]; thus, an increase in the nanoparticle concentration in the base fluid leads to an increase in its viscosity and, consequently, in the pressure drop and pumping power, as shown in Figure 5.

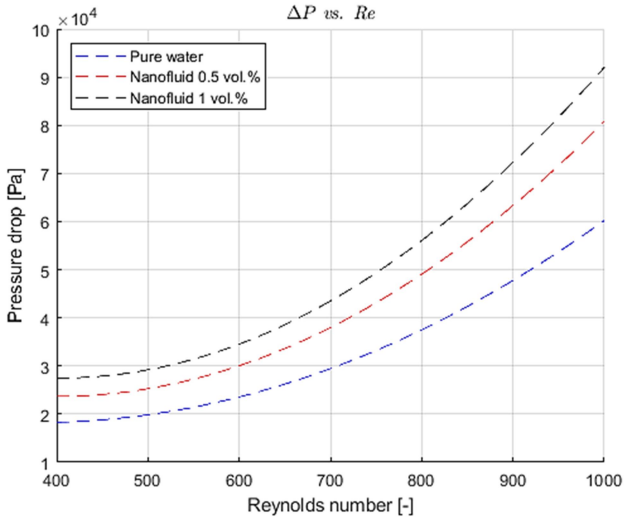

Figure 5. Pressure drop as a function of Reynolds number for Cases 1, 2 and 3, respectively.

The nanofluid with the highest concentration has the highest heat transfer coefficient regardless of the Reynolds number (Figure 6). The nanofluid thermal behavior with the volumetric concentration increasing is probably due to the fluid thermal conductivity increasing, as also mentioned by Jwo et al. [12] and Suresh et al. [13].

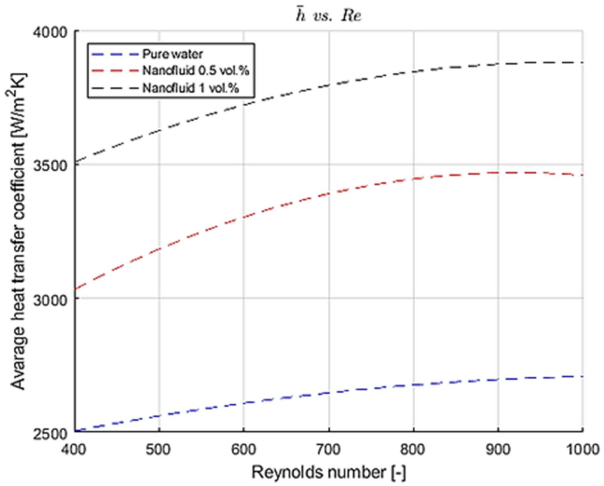

Figure 6. Average heat transfer coefficient for all cases.

4 Conclusions

The numerical analysis developed in this work allowed us to understand that the application of nanofluids results in effective cooling compared to DI-water. The proposed heat sink showed a reduction in wall temperature of around 27.8% when nanofluid was applied. The higher the nanofluid concentration, the lower the wall temperature, and it varies up to 8% as it increases from 0.5 vol.% to 1 vol.%.

A higher pressure drop occurs when nanofluid is used as the working fluid; for Al_2O_3-water nanofluid with 1 vol.%, a 31% increase was found compared to DI-water. Even with the higher pressure drop observed, its effect on the pumping power consumption is acceptable (for the highest nanofluid concentration and Reynolds number, the pressure drop is 93.40 kPa corresponding to a pumping power of 3 W).

The Al_2O_3-water nanofluid improves the heat transfer coefficient regardless of the inlet velocity (for 0.5 vol.%, an increase of around 36% was found compared to DI-water). For the highest nanofluid concentration, the increase in heat transfer compared to pure water represents 43%.

Therefore, the present work numerically shows that AL_2O_3 water-based nanofluid is an effective way of cooling and the combination of microchannels heat sink devices and nanofluids can be used to guarantee efficient cooling to electronic devices.

Acknowledgments. The authors are grateful for the financial support from the PPGEM – UNESP/FEIS, from the National Council of Technological and Scientific Development of Brazil (CNPq grant number 458702/2014-5) and FAPESP (grants numbers 2013/15431-7 and 2019/02566-8).

Authorship statement. The authors hereby confirm that they are the sole liable persons responsible for the authorship of this work and that all material that has been herein included as part of the present paper is either the property (and authorship) of the authors, or has the permission of the owners to be included here.

References

[1] S. S. Murshed and C. N. Castro, "A critical review of traditional and emerging techniques and fluids for electronics cooling". *Renewable and Sustainable Energy Reviews,* vol. 78, n. 1, pp. 821–833, 2017.

[2] W. Qu and Mudawar, "Measurement and prediction of pressure drop in two-phase microchannel heat sinks". *International Journal of Heat and Mass Transfer,* vol. 46, n. 15, pp. 2737–2753, 2003.

[3] M. P. Y. K, Prajapati and M. K. Khan, "Numerical investigation of subcooled flow boiling in segmented finned microchannel". *International Communications in Heat and Mass Transfer,* vol. 86, n. 1, pp. 215–221, 2017.

[4] N. Janjanam, R. Nimmagadda, L. G. Asirvatham, R. Harish and S. Wongwises, "Conjugate heat transfer performance of stepped lid-driven cavity with Al2O3/water nanofluid under forced and mixed convection". Springer Nature, 2021.

[5] M. A. R. S. Al-Baghdadi, Z. M. H. Noor, A. Zeiny, A. Burns, D. Wen, "CFD analysis of a nanofluid-based microchannel heat sink". *Thermal Science and Engineering Progress,* vol. 20, n. 1, 2020.

[6] W. Qu and Mudawar, "Experimental and numerical study of pressure drop and heat transfer in a single-phase microchannel heat sink". *International Journal of Heat and Mass Transfer,* vol. 45, n. 12, pp. 2549–2565, 2002.

[7] H. Tan, L. Wu, M. Wang, Z. Yang and P. Du, "Heat transfer improvement in microchannel heat sink by topology design and optimization for high heat flux processor cooling". *International Journal of Heat and Mass Transfer,* vol. 129, n. 1, pp. 681–689, 2019.

[8] B. Ramos-Alvarado, P. Li, H. Liu and A. Hernandez-Guerrero, "CFD study of liquid-cooled heat sinks with microchannel flow field configurations for electronics, fuel cells, and concentrated solar cells". *Applied Thermal Engineering*, vol. 31, n. 1, pp. 2494–2507, 2011.

[9] A. Bell Drive. *Guide for the verification and validation of computational fluid dynamics simulations.* American Institute of Aeronautics and Astronautics, 2002.

[10] F. Ahmed, M. A. Abir, P. K. Bhowmik, V. Deshpande, A. S. Mollah, D. Kumar and S. Alam, " Computational assessment of thermo-hydraulic performance of Al2O3-water nanofluid in hexagonal rod-bundles subchannel". *Progress in nuclear energy,* vol. 135, n. 1, 2021.

[11] M. Z. U. Khan, E. Uddin, B. Akbar, N. Akram, A. A. Naqvi, M. Sajid, Z. Ali, M. Y. Younis and F. P. G. Márquez, "Investigation of Heat Transfer and Pressure Drop in Microchannel Heat Sink Using Al2O3 and ZrO2 Nanofluids". *Nanomaterials,* 2020.

[12] C. S. Jwo, L. Y. Jeng, T. P. Teng and C. C. Chen, "Performance of overall heat transfer in multi-channel heat exchanger by alumina nanofluid". *Journal of Alloys and Compounds*, vol. 504, n. 1, pp. 385-388, 2010.

[13] S. Suresh, K. P. Venkitaraj, P. Selvakumar and M. Chandrasekar, "Effect of Al_2O_3–Cu/water hybrid nanofluid in heat transfer", *Experimental Thermal and Fluid Science*, vol. 38, n. 1, pp. 54-60, 2012.